The ^{12}C+^{12}C fusion reaction at stellar energies

Xiaodong Tang[1,2,3,*] and *Longhui* Ru[1,2,**]

[1]Institute of modern physics, Chinese Academy of Sciences, Lanzhou, 730000, China
[2]School of Nuclear Science and Technology, University of Chinese Academy of Sciences, Beijing 100049, China
[3]Joint department of nuclear physics, Lanzhou University and institute of modern physics, Lanzhou, 730000, China

Abstract. The carbon fusion reaction is crucial in stellar evolution. Despite six decades of studies, there is still a large uncertainty in the reaction rate which limits our understanding of various stellar objects, such as massive stars, type Ia supernovae, and superbursts. In this paper, we review the experimental and theoretical studies of the carbon fusion reaction at sub-barrier energies. An outlook for future studies is also presented.

1 Introduction

Stars with a mass of more than 8 solar masses and less than 10 solar masses can ignite the ^{12}C+^{12}C fusion reaction and proceed with carbon burning inside of their cores. These stars end up their lives as Ne/O white dwarfs. More massive stars will continue with Ne-, O- and Si-burnings in their cores and shells and eventually become supernovae. During these hydrostatic and explosive burning processes, ^{12}C+^{12}C is one of the primary reactions of the burning processes which shape the stellar evolution and the final nucleosynthesis. The typical temperature ranges span from 0.6 to 2.5 GK [1, 2].

The ^{12}C+^{12}C fusion reaction is considered to be the ignition reaction of type Ia supernova and superburst. In type Ia supernova, the ignition happens in the core of white dwarf typically at T$\sim$ 0.15-0.7 GK. In superburst, the heating sources in the crust of neutron star raise the temperature of the ash and eventually start carbon ignition at a temperature of $\sim$0.5 GK[3]. The ignition conditions mentioned above strongly depend on the ^{12}C+^{12}C reaction rate as well as the treatment of reaction rate estimation in dense matter[4–6].

2 Experimental progress

At sub-barrier energies, the main products of ^{12}C+^{12}C are n, p and α. To obtain the fusion reaction cross section at such energies, two different techniques had been used. One is the particle spectroscopy and the other is the characteristic γ-ray spectroscopy. Patterson[7], Mazarakis[8], Becker[9] and Zickefoose[19] extended the measurements below 2.7 MeV by counting the protons and/or alphas from the fusion reaction process. As energy approaches

*e-mail: xtang@impcas.ac.cn
**e-mail: rulonghui@impcas.ac.cn

the astrophysical region, backgrounds arising from the target impurity and other sources produce a significant background. Some proton and alpha channels could not be identified, leading to underestimation of the total fusion cross sections. Kettner[10], Aguilera[11] and Spillane[12] measured the cross sections of the characteristic γ-rays of the fusion residues, ^{23}Na, ^{20}Ne and ^{23}Mg. Since some decays of the fusion residues bypass the decay of the characteristic γ-rays, the sum of the characteristic γ-ray cross sections reflects only a fraction of the total fusion cross section. To get a cleaner background, the particle-γ coincidence technique has been used to measure the cross section of the p_1 and α_1 channels [13–15]. But the statistics was limited by the lower detection efficiency and the available beam current. The total fusion cross section can only be obtained by the theoretical branching ratios which introduce systematic uncertainties as shown later in this paper. A recent direct measurement of ^{12}C(^{12}C,n)^{23}Mg has been performed at stellar energies, providing a reliable rate[16]. The ^{12}C(^{12}C,^{8}Be)^{16}O is an open channel that has been overlooked due to the lack of experimental work[17]. The results of some measurements are shown in Fig. 1 as the modified S factor, $S^*(E_{c.m.}) = \sigma(E_{c.m.})E_{c.m.}exp(\frac{87.21}{\sqrt{E_{c.m.}}} + 0.46E_{c.m.})$.

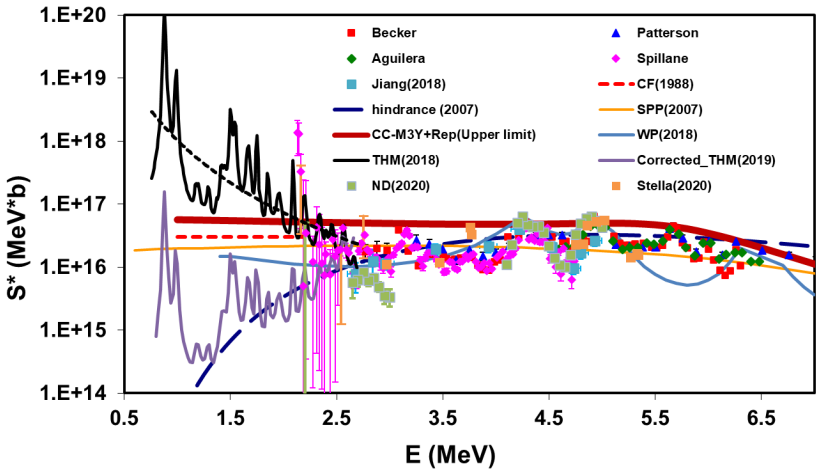

Figure 1. (Color online) S* factors of ^{12}C+^{12}C. The ^{12}C+^{12}C data from Ref. [7], [9], [11], [12], [14] and [15] shown as blue, red, green diamond, magenta, blue, green square and orange points, respectively. Model calculations, CC-M3Y+Rep (thick dark red), SPP(oragen), TDWP(light blue) and hindrance(blue dashed) are also shown, respectively. The recommended averaged S* factor by CF88 is shown as red dashed line. The THM result and the fit are shown as black dashed and solid lines, respectively.

3 Data compilation

Here we discuss three important factors in the compilation of the S* factor of the ^{12}C+^{12}C fusion reaction: energy calibration, background evaluation and the branching ratios of the observed/missing channels.

An accurate and precision energy calibration is the basic to compare the data set. Due to the Coulomb barrier tunneling effect, the reaction cross section has a strong dependence on the reaction energy. For example, at $E_{\rm c.m.}$=3 MeV, a 0.2% change in $E_{\rm c.m.}$ results in a 5% change in the reaction cross section. The measurement of Mazarakis found an upturning trend of the S* factor at the lower energies. It was interpreted as absorption under the

Coulomb barrier. By aligning the resonances at higher energies with latter measurements, an energy shift of +100 keV was found for the data of Mazarakis and the upturning trend disappeared[10, 20].

Barrón-Palos *et al*. reported an upturning trend in their measured S* factor. As they used a smoothing procedure to wash out the resonance structure, one can not check their energy calibration with the reported S* factor. We compared the thick target yields of the 1634-keV transition measured by Spillane *et al*. and Barrón-Palos *et al*.. The result is shown in Fig.2. Although the resonant peaks in the two measurements seem to be aligned with each other, the measurement of Barrón-Palos *et al*. is generally higher than the measurement of Spillane *et al*. except the agreement around the resonance at $E_{c.m.}$=3.2 MeV. For example, the thick target yield of Barrón-Palos *et al*. at $E_{c.m.}$=2.4 MeV is more than a factor of 10 higher than the measurement of Spillane *et al*., resulting in the upturning trend of the S* factor at astrophysical energies. Such a discrepancy may arise from the unknown backgrounds. The strong resonance reported by Spillane *et al*. has not been confirmed by any experiment yet. It will be useful to re-do the measurement, clarify the discrepancy and draw conclusion on the resonances at stellar energies.

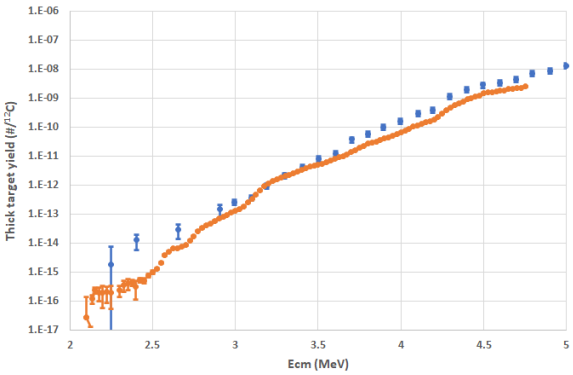

Figure 2. (Color online) Comparison of the thick target yields of the 1634-keV transition measured by Barrón-Palos *et al*. (blue points) and Spillane *et al*. (orange points).

Limited by the detection capability, some channels have to be missed in every experiment. Lacking systematic studies, the correction of the missing channels has been done in various ways. For example, it was thought that the p_0 and α_0 channels were the only missing channels in the γ-spectroscopy measurement[11]. We have performed a systematic analysis to investigate the fractions of missing channels based on a statistical model [21]. In this study, the spin population of the entrance channel was taken from the coupled channel calculation. The decay branching ratio of each channel was evaluated with Talys and calibrated using the experimental data of Becker [9]. Our study shows that the branching ratios of p_1/p_{tot}, γ_{440}/p_{tot}, α_1/γ_{1634}, and $\gamma_{1634}/\alpha_{tot}$ are not constants and the average trends of these branching ratios can be well described with the calibrated statical model prediction. Here p_{tot} and α_{tot} refer to the summed cross sections of the proton and α channels, respectively. We also found the fluctuations around these predictions decrease as the branching ratios increase. Some of the results are shown in Fig. 3. Taking the proton channel as an example, at $E_{c.m.}$=5 MeV, the ratio of p_1/p_{tot} is round 0.2 with a relative fluctuation of 42%(σ) around the prediction. By including more observable channels, the ratio of $\sum_{i=0}^{5} p_i/p_{tot}$ increases to about 0.5 while the corresponding relative fluctuation decreases to 12%(σ). And this relative fluctuation of this

ratio decrease as this ratio increases towards lower energies. Therefore, future experiments are needed to measure as many channels as possible to reduce this systematical uncertainty.

After applying corrections based on branching ratios predicted by the statistical model, the compilation of the experimental S* factors are shown in Fig. 4. An agreement within ±30% is achieved among the total S* factors obtained using the experimental data sets at $E_{c.m.} > 4$ MeV, while some discrepancies remain at lower energies. For example, the recent measurement of α_1 by Tan [14] is about one tenth of the result of Fruet [15] at $E_{\mathrm{c.m.}} < 3$ MeV. Such kind of discrepancies hinder the development of reliable models and should be resolved by better measurements in the near future.

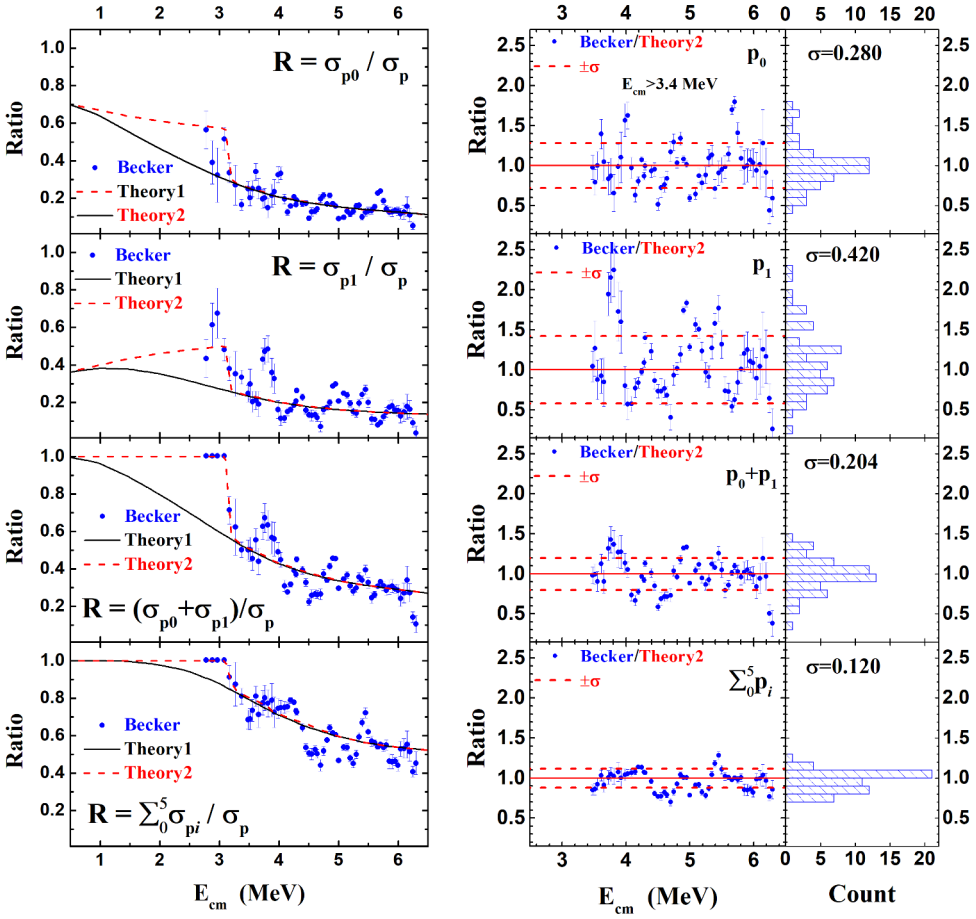

Figure 3. The comparison of the branching ratios calculated with experimental data [9] for the p-channel. (left) The calculated σ_{p_0}/σ_p, σ_{p_1}/σ_p, $(\sigma_{p_0} + \sigma_{p_1})/\sigma_p$, $\sum_{i=0}^{5} \sigma_{p_i}/\sigma_p$ ratios are displayed with experimental data of Becker *et al.* [9]. **Theory1** is the present calculation by Talys, **Theory2** takes the condition of the cut-off exist in the experiment of Becker *et al.* [9] into consideration. (right) The values of Becker/Theory2 for the ratios shown in (left) are calculated and displayed. The statistics are also achieved with average value (Mean=1) and standard deviation (σ). The standard deviation (σ) according to Mean=1.0 is given together with the Becker/Theory2.

Another systematic uncertainty often overlooked is the angular distribution of the detected particles or γ-rays. At the deep sub-barrier energies, as the dominated angular momenta of

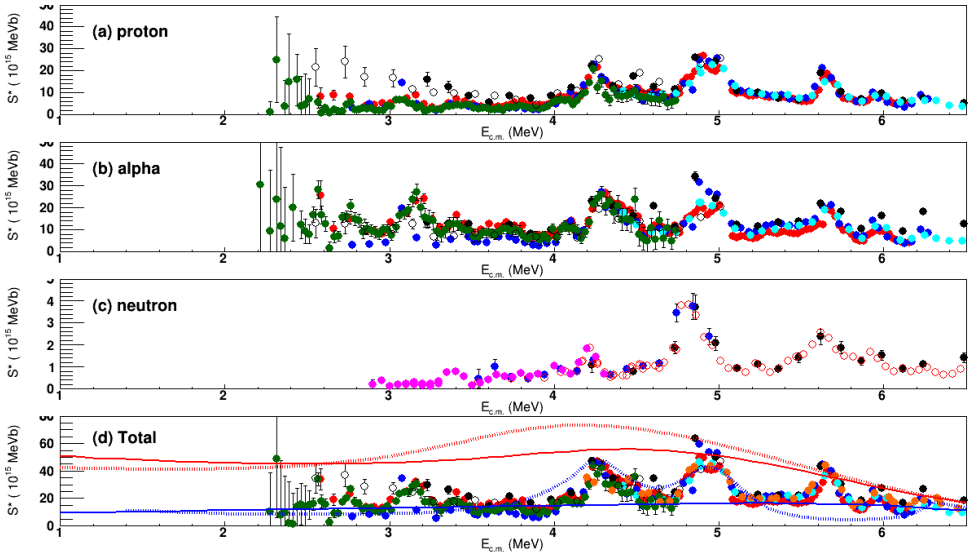

Figure 4. (Color online) The modified S factors of the proton, alpha, neutron channels and their sum are shown as (a), (b), (c) and (d), respectively. The branching ratio corrections have been applied. The explaination of legends can be found in Ref. [21].

the entrance channel are L_i =0 and 2, the angular distribution of the emitted charged particles, p and α, can be anisotropic. The allowed orders of the angular distribution coefficients are 0, 2 and 4. The angular distributions of the exit channels require a complete measurement using a charged particle array and good statistics. They have only been measured by the limited amount of experiments at sub-barrier energies. When the angular distribution coefficient of the fourth order can be ignored, one may approximate the averaged differential cross section by using the differential cross section at 55 or 125 degrees in the center of mass frame. An isotropic angular distribution was assumed to get the integrated cross section. Measurements performed at other angles often use this assumption to determine the integrated cross section, resulting in an unknown systematic uncertainty. More experimental and theoretical investigations are needed to quantify this uncertainty.

4 Test of extrapolating model and the establishment of the upper limit

Modeling ^{12}C+^{12}C heavy ion fusion cross sections at deep sub-barrier energies has been a long standing challenge for nuclear reaction theory [20]. The Gamow energy window for most astrophysical applications typically spans 500 keV or more, and with no reliable method for predicting the resonances at lower energies, the standard reaction rate (CF88) was established by modeling the averaged S* factor,$S^*(E) = S(E)exp(0.46E)$, with a constant value corresponding to a S(E) with a rising trend towards lower energies [7, 22]. The rising trend of S-factor towards lower energies is supported by various phenomenological and microscopic models, such as density-constrained time dependent Hartree-Fock method (DC-TDHF) [23], wave-packet dynamics (TDWP) [24], barrier penetration model based on the global São Paulo potentials (SPP) [5] or the Krappe-Nix-Sierk potential (KNS) [11], and coupled channel calculations [25, 26] such as CC-M3Y+Rep (Fig. 1(a)). However, the hindrance model, a global

phenomenological model based on the systematics observed in systems with 64≳A≳30, predicts that the ^{12}C+^{12}C S-factor reaches its maximum at $E_{\mathrm{c.m.}}$=3.68±0.38 MeV [13, 27–29]. At lower energies, this model predicts a rapid drop in the S-factor leading to a reduced reaction rate that is many orders of magnitude smaller than the standard rate used for astrophysical modeling. However, the complicated resonant structure makes it difficult to test the predictive power of the extrapolating models. As we demonstrated in Fig.5 and Table 1, all the models yield similarly poor reduced-χ^2s of about 5−9.5. Recently, the cross sections were determined indirectly for $E_{\mathrm{c.m.}}$= 0.8 MeV to 2.7 MeV using the Trojan Horse Method [30], recommending a new S-factor with a slope rising faster than any models presented in Fig. 1, resulting in a new rate which is 1 or 2 orders of magnitude higher than the standard one. The large uncertainty of the ^{12}C+^{12}C rate drastically impacts a number of models such as late-time massive star evolution, the ignition dynamics of type Ia supernovae and x-ray superbursts [5, 6].

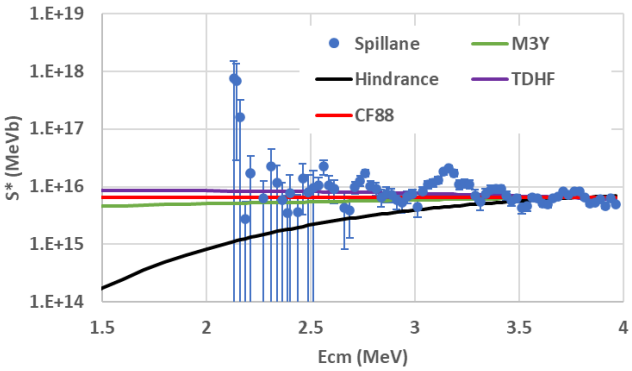

Figure 5. (Color online) The best fits of various models to the experimental S* factor of Spillane in the range of $E_{\mathrm{c.m.}}$= 2.68 to 3.97 MeV. The resulting reduced-χ^2 for the models, M3Y-Rep, Hindrance, TDHF, and CF88, are listed in Table 1.

Table 1. The reduced-χ^2 for different models (scenario 1: No normalization; scenario 2: with renormalization;)

Models	M3Y-Rep	Hind	TDHF	CF88
scenario 1	1888	680	3232	915
scenario 2	6.69	9.47	5.03	6.01

While the complicated resonance-like structure in ^{12}C+^{12}C and the lack of reliable measurements at lower energies prevent us from drawing a clear conclusion [13], the isotope fusion reaction ^{12}C+^{13}C offers an ideal opportunity to constrain the ^{12}C+^{12}C S-factor. It has been observed at energies below and above the Coulomb barrier that ^{12}C+^{13}C and ^{13}C+^{13}C cross sections are upper bounds of the ^{12}C+^{12}C cross sections, and match the maxima of the resonance-like structure seen in ^{12}C+^{12}C in a wide range from 10^{-8} b to 1 b [31]. This strong correlation among the three systems has been well explained by coupled channel calculations and the significantly different level densities of the compound states [32]. At sub-barrier energies, the valence neutron(s) in ^{12}C+^{13}C and ^{13}C+^{13}C increase the level densities of their compound states by at least one order of magnitude in comparison to ^{12}C+^{12}C and result in

smooth cross sections. According to the following equation [32],

$$\sigma = \sum_J \sigma_{cc}^J \left(1 - exp(1 - 2\pi\overline{\Gamma}_J/D_J)\right), \quad (1)$$

the upper limit of the ^{12}C+^{12}C cross section is reached using the high level density limit and can be modeled consistently with the other C+C isotope systems [32]. The average of the ^{12}C+^{12}C fusion cross section is also predicted by modulating the upper limit with the averaged ratio of the level width <Γ> and the level spacing <D> of ^{24}Mg [32]. Since the effect of $< \Gamma/D >$ is not sensitive to the energy, the shape of the averaged cross section is essentially determined by the model used for the upper limit prediction. Therefore, a model well constrained by ^{12}C+^{13}C is crucial for us to set a reliable upper limit and constrain the shape of the averaged cross section for ^{12}C+^{12}C.

We performed an activity measurement in SLANIC mine for the ^{12}C+^{13}C system with energies down to $E_{\mathrm{c.m.}}$=2.323 MeV, at which the ^{12}C(^{13}C,p)^{24}Na cross section is found to be 0.22(7) nb. The ^{12}C+^{13}C fusion cross section is derived with a statistical model calibrated using experimental data. Our result of the ^{12}C+^{13}C fusion cross section provided the first decisive evidence in the carbon isotope systems which rules out the existence of the astrophysical S-factor maximum predicted by the phenomenological hindrance model, while confirming the rising trend of the S-factor towards lower energies predicted by other models, such as CC-M3Y+Rep, DC-TDHF, KNS, SPP and ESW. After normalizing the model predictions with our data, a more reliable upper limit is established for the ^{12}C+^{12}C fusion cross sections at stellar energies [33]. However, this upper limit is lower than the strong resonance observed by Spillane at 2.14 MeV and the indirect THM measurement based on the PWIA assumption. Experimental and theoretical efforts are needed to resolve the issues.

5 Extrapolation towards stellar energies and Reaction Rate

We proposed a new extrapolation based on the lower and upper limits for the S* factor of ^{12}C+^{12}C in parallel to the other existing extrapolation [21]. The KNS extrapolation based on the non-resonant component of the existing S* at higher energies is one of the lower limits we considered. The current TDWP approach does not include the cluster effect which may account for the resonances at deep sub-barrier energies. Therefore it can provide the other lower limit. It is interesting to note that the TDWP calculation agrees with the empirical lower limit (KNS) with a deviation below 33% at energies below 3 MeV. Combining our upper limits with the lower limit based on the prediction of TDWP, the ^{12}C+^{12}C S* factors are better constrained despite the unknown resonances within the unmeasured energy range as shown in Fig. 4(d). The reaction rate of ^{12}C+^{12}C was calculated with the measured S* factors at E≥2.7 MeV, where a reasonable agreement among the experimental total S* factors exists, and using the random S* factor limited by the lower and upper limits for <2.7 MeV. The average of these two limits is used to estimate the mean value of the S* factor. The resulting reaction rates are shown in Fig. 6 together with the rates obtained with the hindrance model and the THM indirect measurement.

6 New approaches

The precise measurement of the tiny reaction cross section demands new experimental techniques with lower background, higher detection efficiency and higher luminosity. The measurement of the channels with the γ-ray emissions is being planned at the LUNA underground laboratory. Jingpin Underground Nuclear Astrophysics collaboration (JUNA) is also pushing

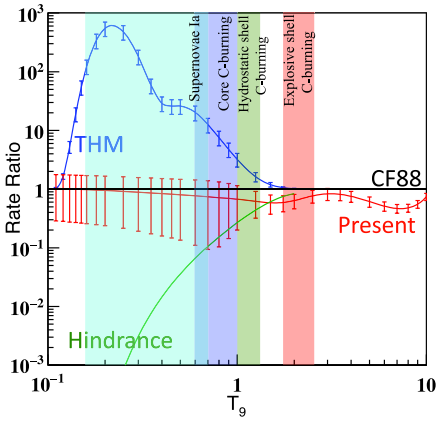

Figure 6. The relative reaction rate obtained in the current work (Red) together with the rates based on the THM measurement [30] (Blue) and hindrance model [28] (Green) to the CF88 rate [22]. Temperatures for core carbon burning (T = 0.6-1.0 GK), hydrostatic shell carbon burning (T = 1.0-1.2 GK), and explosive shell carbon burning (T = 1.8-2.5 GK) are marked by colored bands.

the project of upgrading their accelerator to study the heavy ion fusion reactions at stellar energies. As a complementary approach, we are developing a charged-particle measurement based on the Low Energy Accelerator Facility (LEAF) at IMP [34]. Using the state of art LINAC and powerful ECR sources, LEAF has delivered 50-pμA carbon beam on target, the highest beam intensity ever realized in the carbon fusion experiments. We plan to reach 100 pμA by optimizing the transmission efficiency. To suppress the beam induced backgrounds and the natural background, we developed a new experimental technique using the Time Projection Chamber. With the supreme tracking capability and particle identification, the preliminary thick target yield of ^{12}C(^{12}C,α_0)^{20}Ne has been determined to 1.4(1.4)E-17 evt/^{12}C at $E_{\mathrm{c.m.}}$=2.22 MeV. We are planning to check the strong resonance reported at $E_{\mathrm{c.m.}}$=2.14 MeV in the near future.

The indirect measurement like THM offers a way of extrapolation. But this approach needs to be validated with the direct measurement before applying it at the deep sub-barrier energies [35]. Lacking reliable information of the resonances at deep sub-barrier energies, extrapolating models are not able to provide more precise extrapolation. It has been pointed out theoretically that the molecular resonances in the channel of ^{12}C+^{12}C can be populated via the isoscalar transitions. Therefore, the ^{24}Mg(α,α')^{24}Mg* offers another opportunity to access the resonances at the deep sub-barriers which is not accessible by direct measurement. Such measurements carried out at RCNP [36] and iThemba will provide the important nuclear structure information for the extrapolation at stellar energies.

7 Summary

The ^{12}C+^{12}C reaction is one of the most important reactions in stellar evolution. Despite some progress being made in recent years, there is no satisfactory answer yet for the reaction rate to be used in the astrophysical models. Reliable measurement of the major reaction channels of ^{12}C+^{12}C at energies below 3 MeV, complimentary indirect measurements and standardized data compilation are essential to resolve the existing discrepancies and guide the theory towards the right direction. New experimental and theoretical approaches are

being developed to push the measurement further at deep sub-barrier energies and model the complicated resonance beyond the reach of measurement. With all these efforts, one expects to achieve a more reliable reaction rate for the interest of astrophysics.

8 Acknowledgment

This work was supported in part by the National Key Research and Development Program of China (No. 2016YFA0400501), the Strategic Priority Research Program of Chinese Academy of Sciences (No. XDB34020200).

References

[1] S. Woosley, A. Heger, and T. Weaver, Rev. Mod. Phys. **74**, p. 1015 (2002)
[2] C. Iliadis, *Nuclear Physics of Stars* (WILEY-VCH Verlag GmbH & Co. KGaA, 2007)
[3] R. Cooper, A. Steiner, and E. Brown, Apj. **702**, p. 660 (2009)
[4] L. R. Gasques, A. V. Afanasjev, E. F. Aguilera, M. Beard, L. C. Chamon, P. Ring, M. Wiescher, and D. G. Yakovlev, Phys. Rev. C **72**, p. 025806 (2005)
[5] L. R. Gasques, Phys. Rev. C **76**, p. 035802 (2007)
[6] K. Mori, M. A. Famiano, T. Kajino, M. Kusakabe, and X.D. Tang, Monthly Notices of the Royal Astronomical Society **482**, Pages L70–L74(2019)
[7] J. R. Patterson, H. Winkler, and C. S. Zaidins, Ap.J. **157**, p. 367(1969)
[8] M.G.Mazarakis and W.E.Stephens, Phys.Rev. C **7**, 1280 (1973)
[9] H.W. Becker, K. U. Kettner, C. Rolfs, and H. P. Trautvetter, Zeitschrift für Physik A **303**, 305–312 (1981)
[10] K. Kettner, H. Lorenz-Wirzba, and C. Rolls, Z. Phys. A **298**, p. 65 (1980)
[11] E. F. Aguilera, P. Rosales, E. Martinez-Quiroz, G. Murillo, M. Fernndez, H. Berdejo, D. Lizcano, A. Gmez- Camacho, R. Policroniades, A. Varela, E. Moreno, E. Chvez, M. E. Ortz, A. Huerta, T. Belyaeva, and M. Wiescher, Phys. Rev. C **73**, p. 064601 (2006)
[12] T. Spillane *et al*., Phys. Rev. Lett. **98**, p. 122501 (2007)
[13] C. L. Jiang *et al*., Phys. Rev. C **97**, 012801(R) (2018)
[14] W.P. Tan *et al*., Phys. Rev. Lett. **124**,192702 (2020)
[15] G. Fruet *et al*., Phys. Rev. Lett. **124**, 192701 (2020)
[16] B. Bucher *etal*., Phys. Rev. Lett. **114**, p. 251102 (2015)
[17] B.Cujec, I.Hunyadi, and I.M.Szoghy, Phys.Rev. C **39**, 1326 (1989)
[18] L. Barrón-Palos *etal*., Nucl. Phys. A **779**, P.318 (2006)
[19] J.Zickefoose *et al*., Phys.Rev. C **97**, 065806 (2018)
[20] C. A. Barnes, S. Trentalange, and S. C. Wu, "Treatise on heavy-ion science," (Plenum Preess, New York, 1985) Chap. 1,, pp. 3–60.
[21] Y. J. Li, X. Fang, B. Bucher, K. A. Li, L. H. Ru and X. D. Tang, Chin. Phys. C **44**, 115001 (2020)
[22] G. R. Caughlan and W. A. Fowler, Atomic Data And Nuclear Data Tables **40**, p. 283 (1988)
[23] K.Godbey, C.Simenel, and A.S.Umar, Phys.Rev. C **100**, 024619 (2019)
[24] A.Diaz-Torres and M.Wiescher, Phys. Rev. C **97**, 055802 (2018)
[25] M. Assuncao and P. Descouvemont, Phys. Lett. B **723**, 355–359 (2013)
[26] H. Esbensen, X. Tang and C.L. Jiang, Phys. Rev. C **84**, 064613 (2011)
[27] B. B. Back, H. Esbensen, C. L. Jiang, and K. E. Rehm, Rev. Mod. Phys. **86**, 317 (2014)

[28] C. L. Jiang, K. E. Rehm, B. B. Back, and R. V. F. Janssens, Phys. Rev. C **75**, 015803 (2007)
[29] C. L. Jiang, B. B. Back, K. E. Rehm, K. Hagino, G. Montagnoli and A. M. Stefanini, Eur. Phys. J. A **57**, 235 (2021)
[30] A. Tumino *et al*., Nature **557**, 687 (2018)
[31] M. Notani *et al*., Phys. Rev. C **85** (2012) 014607
[32] C.L. Jiang *et al*., Phys. Rev. Lett. **110**, 072701 (2013)
[33] N.T. Zhang *et al*., Phys. Lett. B **801**, 135170(2020)
[34] Y. Yang *et al*., J. Phys.: Conf. Ser. **1401**, 01201(2020)
[35] A.M. Mukhamedzhanov, A.S. Kadyrov and D.Y. Pang, Eur. Phys. J. A **56**, 233 (2020)
[36] T. Kawabata *et al*., Few-Body Systems 54, 93 (2013)